Hyperlocal: Inferring Location of IP Addresses in Real-time Bid Requests for Mobile Ads*

Long T. Le[†] Tina Eliassi-Rad[†] Foster Provost[‡§] Lauren Moores[§]
[†]Rutgers University [‡]New York University [§]Dstillery
[†]{longtle, eliassi}@cs.rutgers.edu [‡]fprovost@stern.nyu.edu [§]{foster, lmoores}@dstillery.com

ABSTRACT

To conduct a successful targeting campaign in mobile advertising, one needs to have reliable location information from real-time bid requests. However, many real-time bid requests do not include fine-grained location information (such as latitude and longitude) because (1) the device or the application did not collect that information or (2) some components of the real-time bid ecosystem did not forward that information. In this paper, we present a three-step approach that takes as input hashed public IP addresses in real-time bid requests and (1) creates a weighted heterogenous network, (2) applies network-inference techniques to infer fine-grain (but possibly noisy) location information for the hashed public IPs, and (3) uses k-nearest neighbor and census data to assign census block group IDs to those hashed public IPs. Our experiments on two large real-world datasets show the accuracy of our approach to be over 74% for hashed IPs (regardless of their type: mobile or non-mobile) when basing the inference on only hashed public mobile IPs. This is notable since our inference is over 212K possibilities.

Categories and Subject Descriptors

H.2.8 [**Database Applications**]: Data mining; E.1 [**Data Structures**]: Graphs and networks

General Terms

Algorithms, Design, Performance, Experimentation

Keywords

Location inference; location-based services; mobile mining

1. INTRODUCTION

When targeting advertisements for mobile devices, having reliable, fine-grained location information for real-time bid (RTB) requests is an important part of conducting a successful campaign. However, many RTB requests either do not include location information or the information is too coarse-grained (e.g., it is at the city or zip-code level). In a recent collection of approximately 44 million RTB requests, 37% of them had no location information. Based on the traffic type, the percentage of requests without location information can be as high as 84%.[1] There are many reasons why RTB requests do not have fine-grained location information. These reasons can be divided into two broad categories: (1) the device (e.g., iPhone) or the application (e.g., the Twitter mobile app) did not collect the location information; and (2) one or more components of the RTB ecosystem did not forward this information. Note that due to IP address translation, targeters cannot simply look up fine-grained location of IP addresses in common databases.

We present a fast and scalable approach to solving the problem of inferring locations of (hashed) IP addresses in real-time, mobile bid requests at the Census Block Group (CBG) level. A CBG typically covers a contiguous area and contains between 600 and 3,000 people; the United States is divided into approximately 212K CBGs.[2] Our working assumption is that CBGs comprise location information fine-grained enough for useful *hyperlocal* ad targeting, yet coarse-grained enough to avoid major privacy concerns.

Our proposed approach has three steps. First, we create a weighted heterogeneous "movement" network with hashed IP addresses as nodes. A node u has an edge to a node v if the same device uses u at time t_1 and then uses v at time t_2 (where $t_1 < t_2$)—i.e., the device moves from u at t_1 to v at t_2. The novelties of our movement network are: (a) the separation of mobile and non-mobile IP addresses; and (b) the storing of inter-arrival times (IATs) and number of movements on each edge of the network. Second, we apply local relational classifiers with movement- and IAT-based weights to infer the fine-grained location of the hashed IP addresses without location information. This fine-grained information can be noisy. Third, we assign CBG IDs to the predicted (and possibly noisy) fine-grained location information by using a new procedure that employes k-nearest neighbor and census data. Based on extensive empirical studies, our accuracy on inferring CBG IDs for all hashed IP types is over 74% (when basing the inference on only mobile IPs). This is notable since we are estimating the correct CBG out of approximately 212K possibilities.

The main contributions of our work are as follows:

- We introduce an efficient and effective solution for inferring fined-grained location information for hashed IP addresses in RTB requests. Our solution has three components:

  1. Given RTB requests, we build a weighted heteroge-

*We thank Jason Dolatshahi and William Payne for helping us collect the data and for their useful comments. The design of the method was conducted while all authors were at EveryScreen-Media, now part of Dstillery.

ACM SIGSPATIAL LBSN '13, November 5, 2013, Orlando, FL, USA

[1]Nowadays, traffic from mobile applications tend to have more location information.
[2]`http://census.gov`

neous movement network among hashed public IP addresses.

2. We employ local network-inference techniques with weights based on the number of movements and the inter-arrival time distributions to predict latitude and longitude values for hashed public IP addresses with no location information.
3. We introduce a k-nearest neighbor procedure to assign CBG IDs to predicted (and possibly noisy) latitude and longitude information inferred in Step 2.

- We demonstrate the effectiveness of our approach on two large real-world datasets with millions of RTB requests and observe an accuracy of over 74% for all hashed IP types (mobile and non-mobile) when basing the inference on only hashed public mobile IP addresses. Our results are noteworthy since we are inferring the correct CBG out of approximately 212K possibilities.

The paper is organized as follows. Next we discuss background and related works. In Section 3, we introduce our proposed method. Section 4 presents our experiments and discussion. We conclude the paper in Section 5.

2. BACKGROUND AND RELATED WORK

The ecosystem for mobile RTB advertisement has the following seven major components (which form a chain): (1) *Advertisers* such as Nike, (2) *Trading Desks* such as Cadreon, (3) *Demand-Side Platforms* such as Adform, (4) *Ad Exchanges* such as DoubleClick, (5) *Supply-Side Platforms* such as Admeld, (6) *Publishers* such as NY Times, and (7) *Consumers*.[3] The datasets used in our work consist of RTB requests, which were collected from various popular Supply-Side Platforms (a.k.a. SSPs).

Accurately inferring the location of an IP address is important in many applications. To the best of our knowledge, this work is the first of its kind that uses just the structure of an IP×IP movement graph to infer locations, in terms of Census Block Group IDs, for hashed public IP addresses. Wong et al. [9] propose a framework for locating IPs by representing node positions through regions, expressing constraints as areas, and computing locations by solving a system of geometric constraints. In another study, Wang et al. [8] develop a client-independent geolocation system. Both of these methods rely on pings to estimate the round trip time between two machines. They also rely on landmarks, which are collected manually. Our approach does not have these limitations.

Balakrishnan et al. [1] study geolocating IP addresses on mobile networks. They examined the properties of cell-phone IP addresses. Their study showed that mobile IPs are ephemeral and their addresses are itinerant. For example, an individual cell phone can report different IP addresses to various servers within a short period of time. This phenomenon makes it very difficult to track mobile devices without having any software on them, which is our scenario. Furthermore, the same public IP address is often used by many devices. Metwally et al. [5] estimate the number of users of an IP address by keeping track of the application-specific traffic, which can be costly.

There are previous studies that use social interaction to model user movement and predict the future location of a user [2], [6], [3]. These methods require information about the social relations between users through phone calls or friendships on an online social network. In our work, we do not have access to such information.

[3]A nice picture of this ecosystem is available at `http://eliassi.org/businessinsider_mobile_rtb.pdf`.

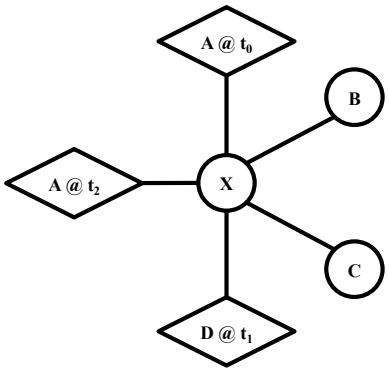

Figure 1: A small sample of an IP×IP movement graph. The circle nodes are non-mobile IPs. The diamond nodes are mobile IPs. The mobile IPs are time-stamped because they are transient. To avoid clutter, we do not show the weights on edges, which are the number movements between two nodes and the inter-arrival times for all movements on an edge.

3. PROPOSED METHOD

Before we start this section, it is important to note that the IP address which one finds when one looks up the address from one's computer (e.g., via `ipconfig`) is **not** the IP address that is seen in an RTB request. An address translation is done between the two, which results in a public IP address, provided by the Internet Service Provider. This public IP is the address that the outside world sees (e.g., a Web server sees when one logs into its Web site). These public IP addresses are then hashed.

Our proposed method has three steps: (1) building IP×IP movement graph, (2) employing local relational classifiers to infer fine-grained (and possibly noisy) location information, and (3) assigning Census Block Group (CBG) IDs as proxies for location.

3.1 Building the IP×IP Movement Graph

Given that we are interested in inferring the location of an IP address, we represent the RTB requests as a network of movements between heterogenous IP nodes.[4] In particular, we have two different types of IP addresses: mobile and non-mobile. Examples of mobile IP addresses are ones with connection types 3G, 4G, LTE, etc. Examples of non-mobile IP addresses are ones with connection types broadband, xDSL, cable, etc. Figure 1 shows a small sample of an IP×IP movement graph.

Figure 2 illustrates how we determine the type of an IP address. We initially relied on a 3rd party database to classify mobile and non-mobile nodes. However, we noticed that a non-negligible percentage of the IPs classified as non-mobile by the 3rd party database appeared outside of a radius r in 24 hours, which is a characteristic trait of a mobile IP (see Section 4). So, we added an extra condition on whether an IP is non-mobile (i.e., did the IP appear outside radius r in 24 hours?). We attempted various radius values in our experiments (See Section 4). However, the default setting for r is 100m because of the following reasoning. Non-mobile devices use Wi-Fi routers to access the Internet. The range of Wi-Fi routers depends on the routers' antenna technology and surrounding condition. The range of current routers is normally less than 100m.[5]

Two IP nodes, A and B, have an edge if the same network ex-

[4]We use the terms 'network' and 'graph' interchangeably.

[5]For more details, see `http://compnetworking.about.com/cs/wirelessproducts/f/wifirange.htm`.

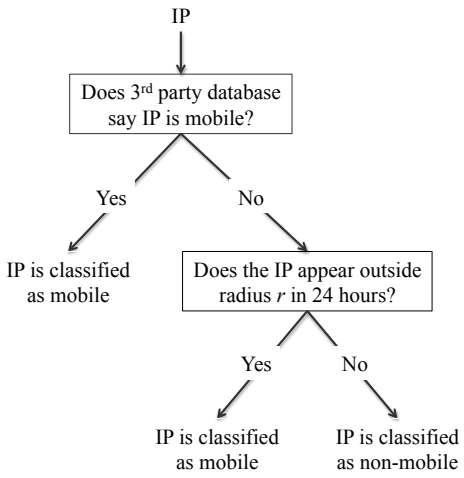

Figure 2: Decision procedure for determining if an IP address is mobile or non-mobile. The extra condition on whether an IP is non-mobile is added because mobile IP addresses tend to change position more quickly than non-mobile IP addresses [1]. The default value for r is 100m (which is the range of current router technology).

change identifier[6] (a.k.a. NUID) uses A at time t_1 and then uses B at time t_2 (where $t_1 < t_2$). Since we are using IP addresses as proxies for locations, a mobile IP address A at time t_i is represented by a node $\langle A, t_i \rangle$ and a non-mobile IP address B at time t_j is represented by B only (see Figure 1). This asymmetry is due to mobile IP addresses being more transient than non-mobile IP addresses.

The inter-arrival time of an NUID's movement from A at t_1 to B at t_2 is stored on the edge. We distinguish between three different types of movements: (1) movement between two non-mobile IP addresses, (2) movement between a non-mobile IP and a mobile IP address, and (3) movement between two mobile IP addresses. In the last case, two mobile IPs are represented by a tuple $\langle A, t_1 \rangle$ and $\langle B, t_2 \rangle$; and, we only consider this a movement if A is different from B. We stress this condition since there are cases where one NUID is involved in two consecutive RTB requests from the same hashed mobile IP address. For example, at time t_1 we observe an RTB request involving an NUID u at hashed mobile IP address A and this same NUID u is observed again in another RTB request at time t_2 with the same hashed IP address A. Due to the way we represent the mobile IP addresses, this NUID appears as $\langle A, t_1 \rangle$ and $\langle A, t_2 \rangle$, but we do not consider this as a movement and do not add an edge between them.

There may be multiple movements between two nodes in our IP×IP movement graph. For each edge in our movement graph, we keep track of the number of movements and the inter-arrival times (IATs) on that edge. Number of movements is the number of times that we observe one NUID use the first IP and then change (or move) to using the second IP. The IAT of a movement is the time gap between the appearances of the NUID when it changes from one IP address to another. Since there are multiple movements between IPs, we actually have distributions of IATs over the edges. In our experiments, we only use the minimum IAT of all the movements on an edge since a smaller IAT generally indicates a smaller distance.

[6]A network exchange identifier is associated with each device. This information is not always provided.

3.2 Employing Local Relational Classifiers

When inferring location on the IP×IP movement graph, it is desirable to conduct inference locally. This is because (1) the farther out one moves in the movement graph, the farther away one gets geographically; and (2) the movement graph is often very large so non-local approaches can be computationally burdensome.

For our local relational classifier, we utilize *wvRN*, which stands for *weighted-vote Relational Neighbor* classifier [4]. wvRN estimates class membership probabilities using the assumption of *homophily* (i.e., like attracts like) in the network data. Given the existence of homophily, wvRN performs well when compared to more complex classifiers [4].

The key for our inference problem is what weight to use in wvRN. We consider two weights: (1) number of movements and (2) minimum IAT. We refer to the former as `wvRN(numMoves)` and the latter as `wvRN(minIAT)`.

`wvRN(numMoves)` uses the number movements between two IP addresses as the weight in wvRN. The intuition behind this weight is that a node v will be closer in distance to its neighbors with whom it has more movements. So, w_i is the number of movements between v and its i-th neighbor.

Our IP×IP movement graph, like many other real-world graphs, is very sparse. That is, it has many edges with only one movement. This inspired us to try another weight based on IATs.

`wvRN(minIAT)` uses the normalized minimum IAT between two IP addresses. It makes sense for the IAT to be a good indicator for the distance between two nodes since the longer the IAT, the longer distance the user has potentially moved (sans traffic). We use $\texttt{minIAT}_v$ to denote the minimum IAT on all edges of a node v. Then, the weight on the movement between v and its neighbor i is defined as

$$w_i = \frac{\texttt{minIAT}_v}{\min(t),\ \forall t \in \text{IAT}(v,i)}$$

where $\text{IAT}(v, i)$ returns the list of IATs between v and i. Note that in the above formula, the denominator is never strictly smaller than the numerator. So, the largest value for w_i is 1, indicating that there was a movement between v and its neighbor i that took $\texttt{minIAT}_v$ time.

wvRN Equations. Given a node v, its neighbors $\text{NBR}(v)$ who have location information, and the weights on the edges between v and its neighbors (where w_i is the weight on the edge from v to its i-th neighbor), we use the following equations to predict latitude and longitude values for v:

$$\text{lat}(v) = \frac{\sum_{i \in \text{NBR}(v)} w_i \times \text{lat}(i)}{\sum_{i \in \text{NBR}(v)} w_i} \ ; \ \text{lon}(v) = \frac{\sum_{i \in \text{NBR}(v)} w_i \times \text{lon}(i)}{\sum_{i \in \text{NBR}(v)} w_i}$$

Restricting Inter-arrival Times on IPs with One Known Neighbor. Like most real-world graphs, our IP×IP movement graph has a skewed degree-distribution (see Figure 6), with many nodes having only one neighbor. By putting a constraint on the IAT of IPs with only one neighbor (e.g., that the IAT has to be less than or equal to 60 min), we can effectively prune the noisy links from the IP×IP movement graph. The only issue here is that with pruning, one also reduces the size of the inference set. We explore this issue in-depth in Section 4.

3.3 Assigning Census Block Groups as Proxies for Location

We infer the location of a hashed public IP address at the *Census Block Group* (CBG) level instead of the ⟨latitude, longitude⟩ level.

The US Census Bureau defines a census block as the smallest geographic unit used in tabulation of data collected from all residences. The US (including Puerto Rico) has about 8.2M census blocks.[7] As the name suggests, a CBG is a group of census blocks, which are close geographically and never cross state or county boundaries. The US (including Puerto Rico) has about 212K CBGs, each containing an average of 39 blocks and between 600 and 3000 people.[8] We decided to infer location at the CBG level because (1) it provides a more consistent labeling for location of IP addresses; (2) it allows incorporation of external data that utilize census data such as demographics; and (3) in the majority of mobile applications (e.g., mobile ads), this level of location information is sufficient for a successful campaign.

Given the predicted ⟨latitude, longitude⟩ of an IP address from `wvRN` (see previous section), we need a method for assigning a CBG ID to it. Our procedure, a k-nearest neighbor approach, is as follows:

Inputs:

- Location of interest, $loc = \langle lat, lon \rangle$
- For each CBG i in the US, i's centroid $c_i = \langle lat_i, lon_i \rangle$ and i's area a_i in km

Output: The CBG ID that contains loc

Procedure:

1. $C \leftarrow$ centroids of the k nearest CBGs to loc
2. For j in C do

   $d_j \leftarrow \text{dist}(loc, c_j)$ // distance between loc and the centroid of the j-th nearest CBG

   $r_j \leftarrow \sqrt{(\frac{a_j}{\pi})}$ // CBG radius of the j-th centroid

   $ratio_j \leftarrow \frac{d_j}{r_j}$ // ratio of distance to radius
3. Return the CBG ID corresponding to $\min(ratio_j), \forall j \in C$

Since we compute the latitude and longitude of an IP based on neighboring IP addresses' latitudes and longitudes, a location may be returned that is in the middle of a lake, forest, or desert. In such cases, the minimum ratio is high; and it is unreasonable to return a CBG ID. Thus, our algorithm will return "unknown" in such cases. Specifically, if the minimum ratio $(\frac{d_j}{r_j})$ is over a threshold t, our procedure returns "unknown" for the CBG ID of the given IP. In our experiments, the percentage of CBG IDs returned as "unknown" was less than 1% with $k = 5$ and $t = 2$. See Section 4 for details.

4. EXPERIMENTS

This section is organized as follows: data description, experimental setup, results, and discussion.

4.1 Data Description

We conducted experiments on two real-world datasets. Table 1 lists the basic characteristics of each dataset. For our experiments, we only consider RTB requests with valid United States NUIDs. Recall that NUID is the network exchange identifier. Each device has an NUID; but it is not always in the RTB request. Also, NUIDs for the same device may be different across different SSPs.

[7] `http://en.wikipedia.org/wiki/Census_block`
[8] These statistics are from the 2000 census.

Data name	Oct-2012	Feb-2013
Collection date	10/01/2012 (Monday)	02/06/2013 (Wednesday)
# of RTB requests with valid USA NUIDs	44.1M	21.5M
% of RTB requests **without** location	36.5%	56.7%
% of RTB requests from **mobile** IPs	57.3%	47.7%

Table 1: Some characteristics of our two datasets: one collected on 10/01/2012 and the other on 02/06/2013. The number of real-time bid requests decreased by about 51% from October 2012 to February 2013 due to reductions from the supply-side providers. However, the number of requests without location information increased by about 55%. The number of requests from mobile IPs decreased by about 17%. We collected data from another day (a Saturday) in February 2013 and the characteristics were similar to 02/06/2013.

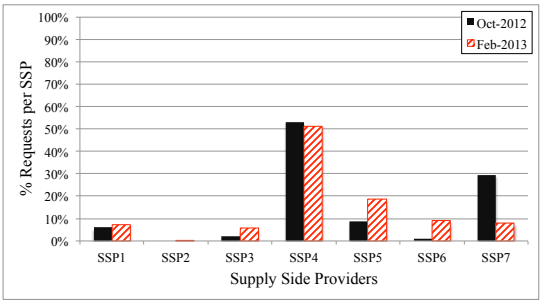

(a) % Requests per SSP

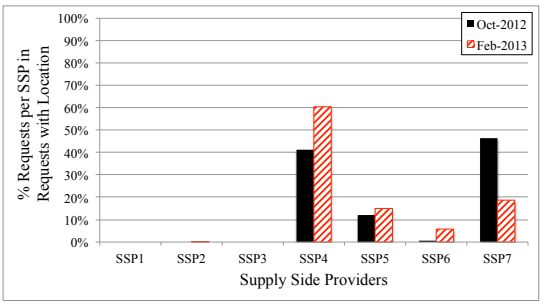

(b) % Requests per SSP in the requests **with** location information

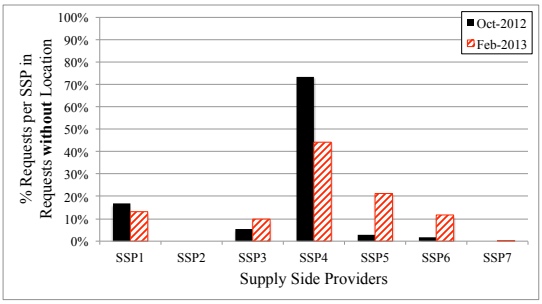

(c) % Requests per SSP in the requests **without** location information

Figure 3: Data characteristics per supply side provider (SSP). (a) SSP4 provides about 50% of the requests for both datasets. (b) Among the requests with location information, SSP4 and SSP7 dominate. (c) Among the requests without location information, SSP4 dominates.

Homophily measured on...	Oct-2012	Feb-2013
All movements	96.5%	90.8%
Mobile to mobile movements	98.6%	99.2%
Non-mobile to non-mobile movements	86.9%	78.1%

Table 2: Homophily in IP×IP movement graphs. Homophily is defined as the number of movements whose (IP) endpoints are from the same SSP divided by the total number of all movements. Homophily levels are high in both datasets. Movements between mobile IPs have very high homophily.

Figure 3 provides details about the datasets such as distribution of RTB requests over SSPs, and the conditional distributions of RTB requests over SSPs given only the requests with location, and then given only the requests without location information. Recall that we may not have location information for a request because (1) the RTB system did not forward it, (2) the SSP did not forward it, (3) the device did not capture it, or (4) the user did not enable location-based services.

Figure 4 shows the distribution of requests with and without location information per SSP. All requests from some SSPs (e.g., SSP1 and SSP3) are without location information. On the other hand, some SSPs (e.g., SSP7) provide location information for all of their requests.

Table 2 reports the amount of *homophily* (i.e., like attracting like) in our IP×IP movement graphs. We define homophily as the number of movements whose (IP) endpoints are from the same SSP divided by the total number of all movements. Homophily is high (greater than 90%) in both datasets. The Feb-2013 data has less homophily (by $\approx 5.7\%$) than the Oct-2012 data. Homophily between mobile IPs is very high (over 98%). Homophily between non-mobile IPs is lower than that of mobile IPs (namely, 86.9% for Oct-2012 and 78.1% for Feb-2013).

Given the high levels of homophily in the IP×IP movements graphs, can we predict location for IPs whose requests are from SSPs without location information? The answer to this question is yes. We observe sufficient non-homophily in the graphs that if an SSP does not have location information for its requests, we can still predict location for its IPs (because its IPs are likely to be linked to other IPs from SSPs with location information). Figure 5 depicts this non-homophily for SSP1 and SSP3, which do not provide any location information for their requests. More than 50% of IPs from these SSPs have movements to IPs from other SSPs (which provide location information).

4.2 Experimental Setup

We show results for `wvRN(minIAT)` and `wvRN(numMoves)` (both described in Section 3.2). Recall that we measure accuracy by checking the predicted CBG ID vs. the actual CBG ID of an IP.

We divide our experiments into nine combinations of: *infer location for X using Y*. Values for X are 'all IPs', 'mobile IPs', and 'non-mobile IPs.' Values for Y are 'all neighbors', 'mobile neighbors', and 'non-mobile neighbors.' As discussed before, these IPs are all public IP addresses that have been hashed.

Figure 6 shows the degree distribution for these nine combinations with all neighbors and with only known neighbors (i.e. neighbors with location information) for the Oct-2012 data. The plots for the Feb-2013 data are similar and were omitted for brevity. We observe that except for degree distribution over mobile IPs, the rest follow power-law distributions with heavy tails. The mobile degree distributions are different because we represent them as time-stamped nodes (as described in Section 3.1).

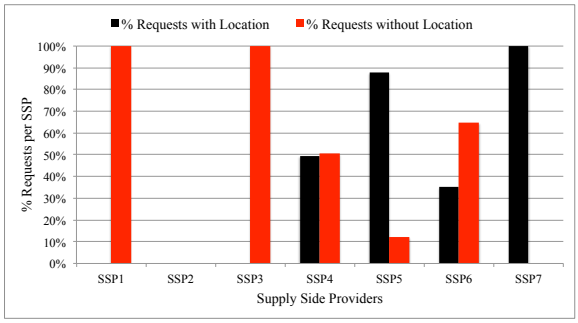

(a) Oct-2012

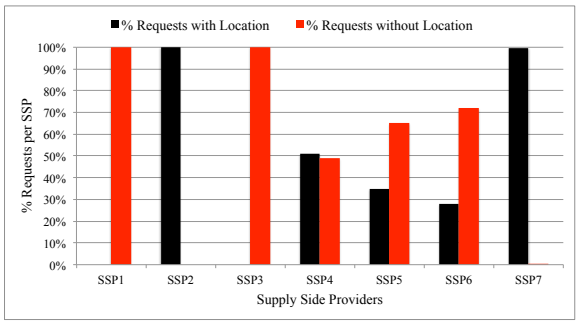

(b) Feb-2013

Figure 4: Percentage of requests with and without location information per SSP. None of the requests from SSP1 and SSP3 have location information. However, all the requests from SSP7 have location information.

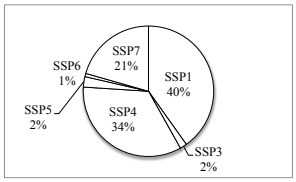

(a) Oct-2012: Movements between SSP1 & other SSPs

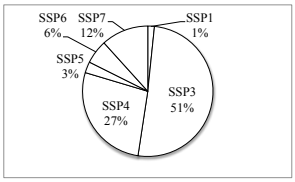

(b) Oct-2012: Movements between SSP3 & other SSPs

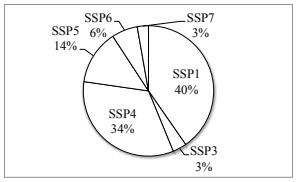

(c) Feb-2013: Movements between SSP1 & other SSPs

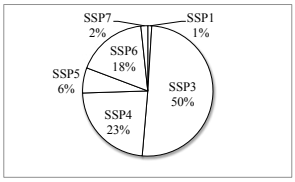

(d) Feb-2013: Movements between SSP3 & other SSPs

Figure 5: Percentage of IPs from SSP1 requests and from SSP3 requests that connect to other SSPs. Recall that none of the requests from SSP1 and SSP3 had location information. We observe that there is a considerable overlap with other SSPs that provide location information.

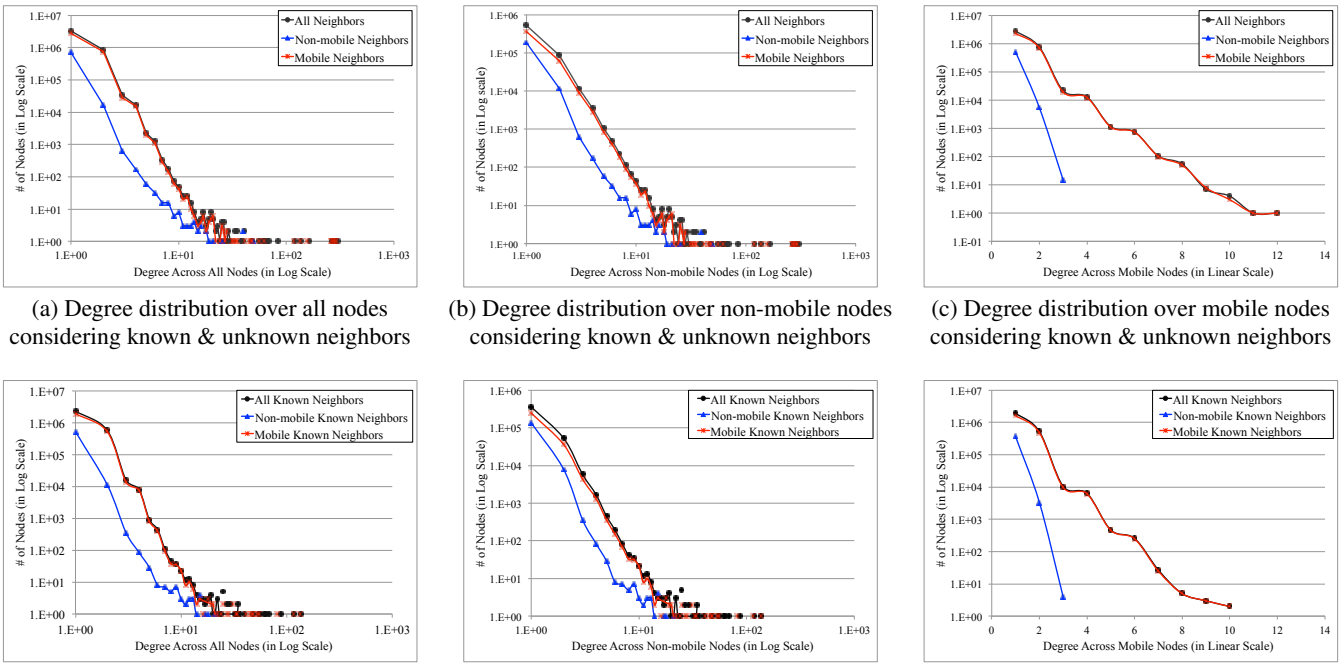

(a) Degree distribution over all nodes considering known & unknown neighbors

(b) Degree distribution over non-mobile nodes considering known & unknown neighbors

(c) Degree distribution over mobile nodes considering known & unknown neighbors

(d) Degree distribution over all nodes, considering only known neighbors

(e) Degree distribution over non-mobile nodes, considering only known neighbors

(f) Degree distribution over mobile nodes, considering only known neighbors

Figure 6: Oct-2012 degree distributions for the various combinations of inferring location for X given Y. Values for X are 'all IPs,' 'mobile IPs,' and 'non-mobile IPs.' Values for Y are 'all neighbors,' 'mobile neighbors,' and 'non-mobile neighbors.' Given how we represent mobile IPs as time-stamped nodes, we expect a different distribution in (c) and (f) than in other plots. The degree-distributions plots for the Feb-2013 data are similar to these plots and are omitted for brevity.

Also, the distributions for all neighbors and known neighbors are very similar. We do not observe sparsity around the neighbors an IP. For example, in the Oct-2012 data approximately 70% of an IP's neighbors are known. Therefore, we do not attempt more computationally expensive relational-learning methods like collective classification [7].

4.3 Results

We ran our experiments on a Macbook Pro with CPU 2.66 GHz Intel Core i7, RAM 8 GB DDR3, hard drive 500 GB SSD, and OS X 10.8. Our algorithm is implemented in Python. We use NetworkX[9] and MongoDB[10] for network management and for finding k-nearest neighbors. It takes us on average 1.2 milliseconds to process each bid request.

Our results are organized as follows: (1) sensitivity to radius r, (2) sensitivity to inter-arrival times, (3) core results, (4), inference over IPs with one known neighbor, (5) inference over IPs with two or more known neighbors, and (6) accuracy with a slack distance.

4.3.1 *Sensitivity to Radius r*

Previously, we illustrated our procedure for deciding whether an IP address is mobile or non-mobile (see Figure 2). We had a radius parameter r, which checked if an IP appeared outside the radius r in 24 hours. What percentage of the IPs do we reverse from the 3rd party decision (i.e., reclassify a non-mobile IP to a mobile IP because it appeared outside the radius r in 24 hours)? Figure 7 answers this question. At the default radius of 0.1km, we respectively reverse 10.5% and 12% of the decisions made by the 3rd party for Oct-2012 and Feb-2013.

How sensitive are our accuracy results to change in the radius parameter? Figure 8 answers this question. We observe that different radii do not significantly change the accuracy of `wvRN(numMoves)`.[11] From a radius of zero to a radius of infiniti, the change in accuracy is less than 10%. In Figure 8, we only plot results for inferring location on (1) all IPs, (2) only mobile IPs, and (3) only non-mobile IPs. In these three cases, we use all neighbors in the inference. The other combinations of this experiment (e.g., infer location of non-mobile IPs using non-mobile neighbors, infer location of non-mobile IPs using mobile neighbors, etc) show the same pattern, so we have omitted them for brevity. For the rest of the experiments, we use a radius r of 0.1km (or 100m). In Section 3.1, we gave a technical reason for using $r = 0.1$km as the default value.

4.3.2 *Sensitivity to Inter-arrival Times (IAT)*

Figure 9 shows accuracy and number of predictions as we vary IAT. We use `wvRN(numMoves)` for inference. The plots show the results on inferring location for all IPs using all neighbors and for non-mobile IPs using all neighbors. The values for mobile IPs are similar to all IPs and are omitted from the plot. The results for the other combinations of infer on X using Y neighbors are also similar and are omitted for brevity. We observe that as IAT is restricted to smaller values, the number of predictions has a bigger drop (relatively speaking) than the gain in accuracy. These results inspired us to use IATs as weights in `wvRN`; and so we developed

[9] `http://networkx.github.io`
[10] `http://docs.mongodb.org`

[11] In this version of wvRN(numMoves), we did not limit IATs for IPs with one known location.

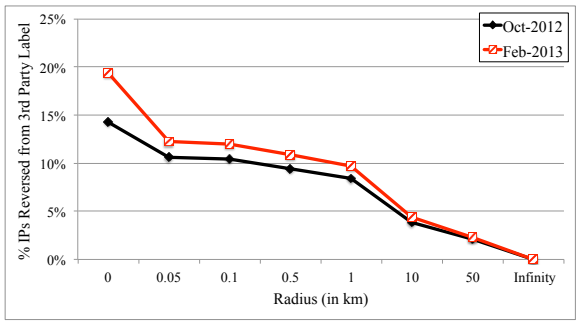

Figure 7: Percentage of IPs whose classification we reverse from the 3rd party decision (see Figure 2 for the decision procedure). A radius of infinity means no constraint was assigned. At our default radius of 0.1km, we reverse 10.5% of the classifications for the Oct-2012 data, and 12% for the Feb-2013 data.

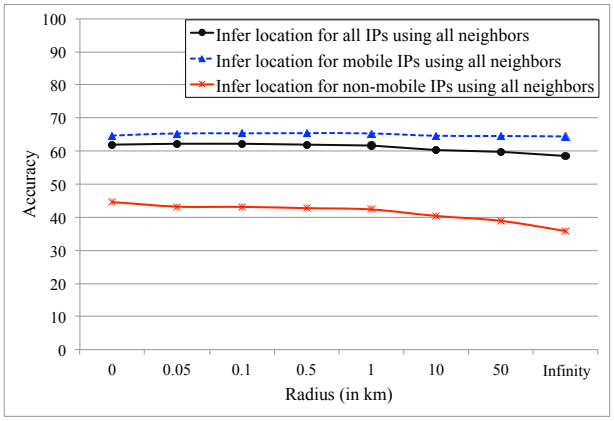

(a) Oct-2012: Accuracy vs. Radius

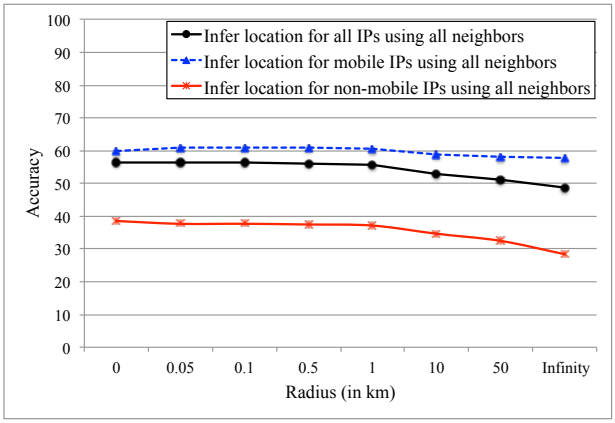

(b) Feb-2013: Accuracy vs. Radius

Figure 8: Sensitivity of `wvRN(numMoves)` to various radii in the decision procedure for mobile vs. non-mobile classification (see Figure 2). A radius of infinity means no constraint was assigned. The trends in the two datasets are the same. In Oct-2012, the maximum difference is an 8% decrease in accuracy between a radius of 0 and a radius of infinity, which appears when we are inferring location for non-mobile IPs using all neighbors (the red plot). The same holds true for Feb-2013, but the maximum difference is about 10%.

the `wvRN(minIAT)` method.

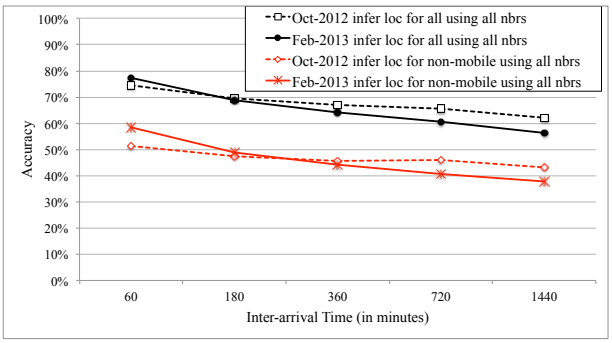

(a) IAT vs. Accuracy

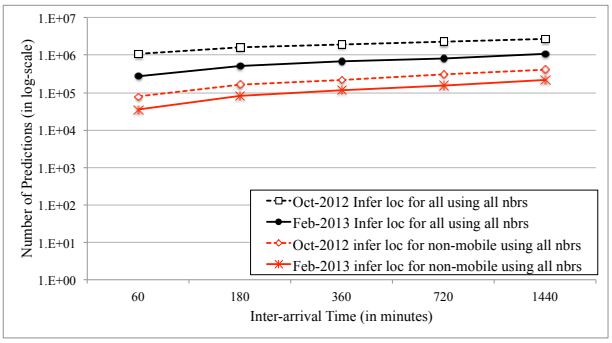

(b) IAT vs. Number of Predictions

Figure 9: Accuracy and number of predictions across different IATs. `wvRN(numMoves)` was used for these experiments. As IAT is restricted to smaller values, the number of predictions has a sharper drop (relatively speaking) than the gain in accuracy. The results on Oct-2012 and Feb-2013 datasets are similar. The Feb-2013 has less predictions because it is a smaller dataset. Radius $r = 100$m.

4.3.3 Core Results

Table 3 reports our core results in terms of (1) accuracy of `wvRN(minIAT)` vs. `wvRN(numMoves)`, (2) number of predictions made (i.e. size of the inference set), and (3) percentage of mobile IPs in predictions. We show results for what type of IP we are inferring location (namely, all IPs vs. mobile IPs vs. non-mobile IPs) and what type of information we are using (i.e., all neighbors vs. mobile neighbors vs. non-mobile neighbors). Our observations are as follows:

- Even though the accuracy of `wvRN(minIAT)` is higher than that of `wvRN(numMoves)`, this difference is not statistically significant at the 0.05 level.
- Both methods have high accuracy (73% to 79%) on inferring location for mobile IPs and all IPs when using mobile neighbors. In the latter case (when inferring for all IPs), between 87.4% to 93.2% of the predictions are on mobile IPs. The range depends on the particular dataset.
- The best accuracy for non-mobile IPs is 55.4% in Oct-2012 and 62.7% in Feb-2013. This is when we use non-mobile neighbors.
- It is more difficult to infer the location of a non-mobile IP than a mobile IP. This is because mobile IPs tend to have

smaller inter-arrival times and smaller distances than non-mobile IPs. In the Oct-2012 data, 77.1% of the mobile to mobile movements were less than 1km; while only 44.2% of the non-mobile to non-mobile movements were less than 1km. These numbers are similar for the Feb-2013 data.

- The number of non-mobile IPs in the datasets are small compared to mobile IPs. See Table 3. This is an artifact of how we represent the mobile IPs (as unique time-stamped nodes). See Section 3.

4.3.4 *Inference over IPs with One Known Neighbor*

Like many real-world networks, our data is highly skewed w.r.t. its degree distribution, with many IPs having only one known neighbor (see Figure 6). Tables 4 and 5 show `wvRN(numMoves)` results of inference on IPs with only one known neighbor. The former table showcases inference on the neighbors whose IAT is less than or equal to 60 minutes; and the latter table showcases inference on the neighbors whose IAT is greater than 60 minutes. The first observation here is that for IPs with only one known neighbor, restricting IAT to be less than 60 mins improves accuracy by an average of 12% for Oct-2012 and 23% for Feb-2013. The second observation is that the restriction on IAT reduces the number of predictions by an average of 4 times for Oct-2012 and 5 times for Feb-2012.

4.3.5 *Inference over IPs with Two or More Known Neighbors*

`wvRN(minIAT)` and `wvRN(numMoves)` have different results only when we take into account IPs with two or more known neighbors. To tease out this difference, we ran experiments where IP nodes with one known neighbor were not considered. Table 6 lists results for IPs with two or more known neighbors. We observe that the accuracy numbers for `wvRN(minIAT)` are higher than `wvRN(numMoves)`. However, these differences are not statistically significant at the 0.05 level.

4.3.6 *Accuracy with a Slack Distance*

So far, we have considered a correct prediction as one in which the predicted CBG ID is equal to the actual CBG ID. What if we allow some slack in this definition? Suppose we consider a correct prediction as: *the distance between the centroids of the predicted and the actual CBG IDs are within slack kilometers*. Figure 10 shows these results for `wvRN(minIAT)` and different values of slack distance. We observe that in the Oct-2012 data at only 25 kilometers slack (i.e., 15.5 miles), our accuracy is 84%, 86%, and 64%, respectively, for inferring the location of all IPs, non-mobile IPs, and mobile IPs using all neighbors. These accuracy numbers are up from 74%, 77%, and 49%, respectively, when we allowed no slack distance. In the Feb-2013 data at only 25 kilometers slack, our accuracy is 81%, 84%, and 64%, respectively, for inferring the location of all IPs, non-mobile IPs, and mobile IPs using all neighbors. These accuracy numbers are up from 74%, 78%, and 53%, respectively, when we allowed no slack distance. The other combination of runs have similar results and are omitted for brevity.

4.4 Discussion

Figure 11 presents the public IP addresses in our datasets drawn on a US map. The blue dots are the IPs for which our method inferred the correct CBG ID. The red dots are the IPs for which our method inferred the incorrect CBG ID. Our method tends to perform better in city centers.

Our results showed the following. **(1)** `wvRN(minIAT)` has slightly better accuracy than `wvRN(numMoves)`, but this difference is not statistically significant at the 0.05 level. **(2)** Accuracy is not sensitive to the choice of radius r used in determining whether an IP is mobile or non-mobile. Also, based on current router technology, $r = 0.1$km is a reasonable default value. **(3)** Restricting movement edges to those with smaller IATs increases accuracy but at a sharp reduction in the number of predictions. **(4)** When inferring location on all IPs and on mobile IPs, time-stamped mobile neighbors provide the best information in terms of location. We observe accuracy between 74% and 77% in Oct-2012 and between 75% and 79% in Feb-2013, respectively. **(5)** Inferring location for a non-mobile IP is a hard task because non-mobile IPs tend to have larger inter-arrival times and larger distances than mobile IPs. For example, in the Oct-2012 data 77.1% of the mobile to mobile movements were less than 1km; while only 44.2% of the non-mobile to non-mobile movements were less than 1km. Also, the number of non-mobile IPs is comparatively much smaller than the number of mobile IPs in the data (see Table 3). **(6)** Allowing some slack distance (say of only 25km) increases accuracy on average by 11% in Oct-2012 and by 9% in Feb-2013.

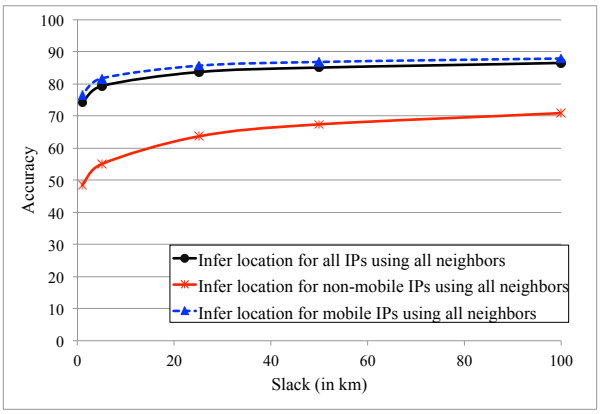

(a) Oct-2012: Accuracy vs. Slack (in km)

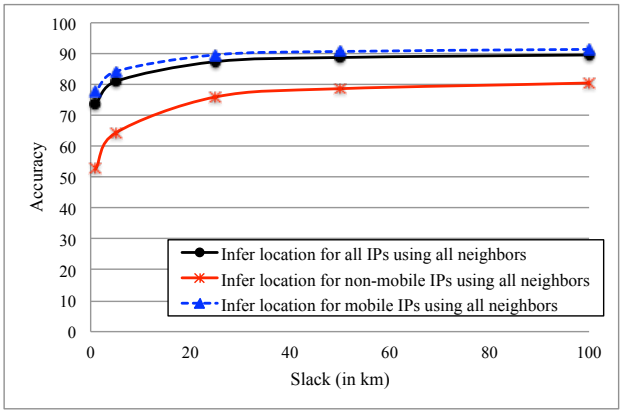

(b) Feb-2013: Accuracy vs. Slack (in km)

Figure 10: Allowing slack distance in computing accuracy, where a prediction is considered correct if the distance between the centroids of the predicted and the actual CBG IDs are within *slack* kilometers. At only 25km slack, accuracy increases by an average of 11% in the Oct-2012 data and 9% in the Feb-2013 data. `wvRN(minIAT)` was used here with radius $r = 100$m.

Infer location for **all** IPs...	Accuracy wvRN(minIAT) Oct-2012 | Feb-2013	Accuracy wvRN(numMoves) Oct-2012 | Feb-2013	Number of Predictions Oct-2012 | Feb-2013	% Mobile in Predictions Oct-2012 | Feb-2013
using all neighbors	71.6 | 70.8	69.7 | 69.3	1,189,679 | 328,015	91.0% | 83.8%
using mobile neighbors	**74.4** | **74.8**	**72.6** | **73.5**	1,077,644 | 278,674	93.2% | 87.4%
using non-mobile neighbors	51.9 | 57.7	51.7 | 57.3	98,338 | 40,777	68.7% | 62.1%
Infer location for **mobile** IPs...				
using all neighbors	74.2 | 75.0	72.3 | 73.6	1,082,566 | 274,900	100% | 100%
using mobile neighbors	**76.6** | **79.1**	**74.7** | **77.9**	1,004,601 | 243,630	100% | 100%
using non-mobile neighbors	50.4 | 54.7	50.2 | 54.5	67,553 | 25,323	100% | 100%
Infer location for **non-mobile** IPs...				
using all neighbors	45.5 | 49.0	44.0 | 46.8	107,113 | 53,115	0% | 0%
using mobile neighbors	44.0 | 45.1	42.5 | 43.0	73,043 | 35,044	0% | 0%
using non-mobile neighbors	**55.4** | **62.7**	**55.0** | **62.0**	30,785 | 15,454	0% | 0%

Table 3: Core results: wvRN(minIAT) vs. wvRN(numMoves). For each method, the highest accuracy values are in boldface. The differences between the two methods are not statistically significant at the 0.05 level. The number of predictions varies depending on the particular inference and the types of neighbors used in the inference process. See Section 4.4 for an explanation of the lower accuracy values when inferring non-mobile IPs or using them in inference. Radius $r = 100$m.

Infer location for **all** IPs with 1 known neighbor with IAT $\leq$ 60min...	Accuracy wvRN(numMoves) Oct-2012 | Feb-2013	Number of Predictions Oct-2012 | Feb-2013	% Mobile in Predictions Oct-2012 | Feb-2013
using all neighbors	72.7 | 76.0	606,274 | 179,294	92.4% | 87.1%
using mobile neighbors	**75.4** | **79.0**	546,498 | 154,610	94.3% | 90.4%
using non-mobile neighbors	52.6 | 59.2	86,981 | 35,073	74.1% | 68.3%
Infer location for **mobile** IPs with 1 known neighbor with IAT $\leq$ 60min...			
using all neighbors	74.7 | 78.7	559,976 | 156,226	100% | 100%
using mobile neighbors	**77.1** | **81.9**	515,575 | 139,714	100% | 100%
using non-mobile neighbors	51.3 | 55.9	64,495 | 23,939	100% | 100%
Infer location for **non-mobile** IPs with 1 known neighbor with IAT $\leq$ 60min...			
using all neighbors	49.1 | 57.5	46,298 | 23,068	0% | 0%
using mobile neighbors	46.9 | 51.5	30,923 | 14,896	0% | 0%
using non-mobile neighbors	**56.3** | **66.5**	22,486 | 11,134	0% | 0%

Table 4: Inference over IPs with one known neighbor and IAT ≤ 60 minutes. The highest accuracy values are in boldface. Restricting IAT to ≤ 60 minutes improves accuracy, respectively, by an average of 12% on Oct-2012 and 23% on Feb-2013; but reduces the number of predictions by an average of 4 times for Oct-2012 and 5 times for Feb-2012. Radius $r = 100$m.

Infer location for **all** IPs with 1 known neighbor with IAT $>$ 60min...	Accuracy wvRN(numMoves) Oct-2012 | Feb-2013	Number of Predictions Oct-2012 | Feb-2013	% Mobile in Predictions Oct-2012 | Feb-2013
using all neighbors	56.3 | 50.7	1,573,436 | 773,095	81.1% | 78.4%
using mobile neighbors	**59.9** | **55.6**	1,262,022 | 594,504	83.6% | 80.9%
using non-mobile neighbors	42.5 | 35.6	369,519 | 207,099	71.0% | 69.6%
Infer location for **mobile** IPs with 1 known neighbor with IAT $>$ 60min...			
using all neighbors	59.5 | 55.2	1,275,406 | 605,948	100% | 100%
using mobile neighbors	**63.0** | **61.7**	1,055,269 | 481,151	100% | 100%
using non-mobile neighbors	43.5 | 31.6	262,188 | 144,226	100% | 100%
Infer location for **non-mobile** IPs with 1 known neighbor with IAT $>$ 60min...			
using all neighbors	42.8 | 34.8	298,030 | 167,147	0% | 0%
using mobile neighbors	**44.2** | 30.0	206,753 | 113,353	0% | 0%
using non-mobile neighbors	40.3 | **44.9**	107,331 | 62,873	0% | 0%

Table 5: Inference over IPs with one known neighbor and IAT > 60 minutes. The highest accuracy values are in boldface. Allowing IAT of > 60 minutes decreases accuracy. This is because IAT on the movement edge is correlated with distance. Generally speaking, the higher the IAT, the larger the distance. Radius $r = 100$m.

Infer location for **all** IPs with $\geq$ 2 known neighbors...	Accuracy wvRN(minIAT) Oct-2012 | Feb-2013	Accuracy wvRN(numMoves) Oct-2012 | Feb-2013	Number of Predictions Oct-2012 | Feb-2013	% Mobile in Predictions Oct-2012 | Feb-2013
using all neighbors	70.4 | 64.6	66.7 | 61.2	583,405 | 148,721	89.6% | 79.8%
using mobile neighbors	**73.4** | **69.7**	**69.6** | **66.7**	531,146 | 124,064	92.1% | 83.7%
using non-mobile neighbors	46.6 | 48.4	44.8 | 45.5	11,357 | 5,704	26.9% | 24.3%
Infer location for **mobile** IPs with $\geq$ 2 known neighbors...				
using all neighbors	73.7 | 70.2	69.7 | 66.9	522,590 | 118,674	100% | 100%
using mobile neighbors	**76.1** | **75.4**	**72.2** | **72.6**	489,026 | 103,916	100% | 100%
using non-mobile neighbors	29.6 | 34.0	26.9 | 30.0	3,058 | 1,384	100% | 100%
Infer location for **non-mobile** IPs with $\geq$ 2 known neighbors...				
using all neighbors	42.7 | 42.6	40.1 | 38.6	60,815 | 30,047	0% | 0%
using mobile neighbors	41.9 | 40.4	39.3 | 36.7	42,120 | 20,148	0% | 0%
using non-mobile neighbors	**52.9** | **53.0**	**51.4** | **50.4**	8,299 | 4,320	0% | 0%

Table 6: Inference over IPs with at least two known neighbors: wvRN(minIAT) vs. wvRN(numMoves). The highest accuracy values are in boldface. The differences between the two methods are not statistically significant at the 0.05 level. The number of predictions varies depending on the particular inference and the types of neighbors used in the inference process. Radius $r = 100$m.

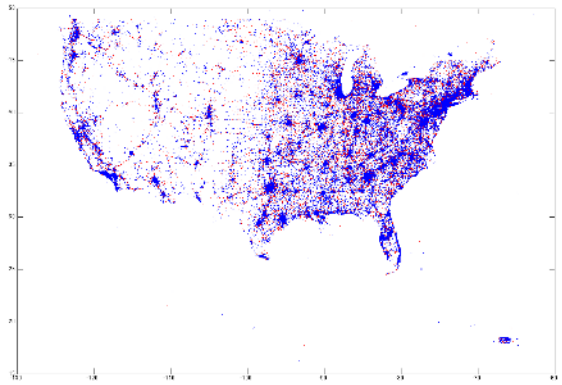

(a) Oct-2012

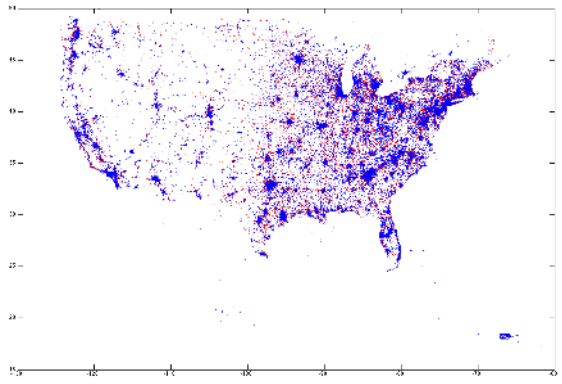

(b) Feb-2013

Figure 11: Hashed IP addresses in our datasets drawn on a US map. The blue dots depict the IPs which our method correctly classified (i.e., inferred the correct CBG ID). The red dots depict the IPs which our method incorrectly classified. Our method tends to be more accurate on IPs in urban centers.

5. CONCLUSIONS

To the best of our knowledge, this work is the first of its kind that uses just the structure of a weighted heterogenous movement graph to infer locations, in terms of CBG IDs, for hashed public IP addresses. We described a novel way of representing hashed IPs in RTB requests either as time-stamped mobile nodes or as non-time-stamped non-mobile nodes. The edges are annotated with the number of movements and the inter-arrival distribution between two IPs. An extensive empirical study on two recent datasets with millions of RTB requests showed that using a local relational classifier (such as wvRN) to infer (possibly noisy) latitude and longitude values and a k-nearest neighbor classifier to infer CBG ID is effective with > 74% accuracy for all IPs. These results are impressive since we are estimating the correct CBG out of 212K possibilities.

6. REFERENCES

[1] M. Balakrishnan, I. Mohomed, and V. Ramasubramanian. Where's that phone? Geolocating IP addresses on 3G networks. In *IMC*, pages 294–300, 2009.

[2] E. Cho, S. A. Myers, and J. Leskovec. Friendship and mobility: User movement in location-based social networks. In *KDD*, pages 1082–1090, 2011.

[3] M. Domenico, A. Lima, and M. Musolesi. Interdependence and predictability of human mobility and social interactions. In *Nokia Mobile Data Challenge*, 2012.

[4] S. Macskassy and F. Provost. Classification in networked data: A toolkit and a univariate case study. *JMLR*, 8:935–983, 2007.

[5] A. Metwally and M. Paduano. Estimating the number of users behind IP addresses for combating abusive traffic. In *KDD*, pages 249–257, 2011.

[6] S. Scellato, A. Noulas, R. Lambiotte, and C. Mascolo. Socio-spatial properties of online location-based social networks. In *ICWSM*, 2011.

[7] P. Sen, G. Namata, M. Bilgic, L. Getoor, B. Gallagher, and T. Eliassi-Rad. Collective classification in network data. *AI Magazine*, 29(3):93–106, 2008.

[8] Y. Wang, D. Burgener, M. Flores, A. Kuzmanovic, and C. Huang. Towards street-level client-independent IP geolocation. In *NSDI*, 2011.

[9] B. Wong, I. Stoyanov, and E. G. Sirer. Octant: A comprehensive framework for the geolocalization of Internet hosts. In *NSDI*, 2007.